

# Monitoring the Concentration of Carbon Dioxide by Measuring the Change in the Resistance of TiO<sub>2</sub> Nanowires Doped with Potassium

Chris Lee

Received March 09, 2024

Accepted April 10, 2024

Electronic access April 30, 2024

The usage of the gas sensor has been increasing very rapidly in industry and in daily life for various potential applications. In recent years, metal oxide semiconductors have become the primary choice for designing highly sensitive, stable, and low-cost real-life applications-based gas sensors due to their inherent physical and chemical properties. In this study, the K-doped TiO<sub>2</sub> nanowires showed the possibility of use as a sensing material due to their consistent response to the presence of CO<sub>2</sub> gas. The reproducibility of sensor assembly has been proved by testing seven different sensors fabricated using the same procedure. In addition, treatment with H<sub>2</sub> plasma improved the sensitivity of the CO<sub>2</sub> gas sensor made of K-doped TiO<sub>2</sub> nanowires. The sensing mechanism was attributed to electron adsorption to the TiO<sub>2</sub> as a result of CO<sub>2</sub> reduction on the surface of K-doped sites. It reduces the hole accumulation layer due to electron–hole recombination process, so the surface resistance of K-doped TiO<sub>2</sub> increases depending on the amount of CO<sub>2</sub> adsorption. This development suggests opportunities for the fabrication of simple, inexpensive CO<sub>2</sub> microsensors with low power consumption.

## Introduction

Gas sensors have been developed to monitor the presence of carbon dioxide (CO<sub>2</sub>) in the environment because of its significant role in global warming. Recently the partial pressure of CO<sub>2</sub> gas generally ranges from 410 to 420 ppm<sup>1</sup>, it is important to monitor the concentration of CO<sub>2</sub> in the atmosphere in order to understand its impact on climatic change. In addition to its effect on climate change, CO<sub>2</sub> gas also has a significant effect on the corrosion rate of the industrial equipment used in chemical processing and the combustion efficiencies in automotive applications. Because of the prevalence of CO<sub>2</sub> and its numerous negative effects, small, inexpensive, reliable solid-state CO<sub>2</sub> gas sensors with low power consumption have been in high demand for several years<sup>2,3</sup>.

Carbon dioxide is a gaseous chemical compound that is composed of two oxygen atoms that are covalently bonded to a single carbon atom. The central carbon atom is connected to two oxygen atoms, and there are no lone pairs of electrons around the central atom. Therefore, carbon dioxide has a linear geometry, so the angle of the O–C–O bond is 180°, and it is a non-polar molecule.

Despite various approaches for monitoring the concentration of CO<sub>2</sub>, only a limited number of CO<sub>2</sub> sensing materials exist due to the stable chemical properties of CO<sub>2</sub> gas<sup>4</sup>. Currently, the most common type of CO<sub>2</sub> sensor is a potentiometric device that consists of either an Na<sup>+</sup> or an Li<sup>+</sup> electrolyte and alkali metal carbonate sensing electrodes. The potentiometric CO<sub>2</sub> sensors are promising because they show satisfactory EMF

signals over a wide range of gas concentrations at high temperatures<sup>5,6</sup>. Most existing CO<sub>2</sub> sensors are large, bulky devices that involve complicated fabrication processes. Because of its numerous negative effects, small, inexpensive, reliable solid-state CO<sub>2</sub> gas sensors with low power consumption have been in high demand for several years<sup>2,3</sup>.

To overcome the disadvantages of potentiometric CO<sub>2</sub> sensors, measurable interaction has been studied. It is related to a surface reaction caused by adsorption–desorption, which leads to a change in the electrical conductance (or resistance) of metal oxides as a result of the charge-carrier transfer<sup>7</sup>. The surface reaction of metal oxide sensors is driven by many factors, such as semiconducting nature (n-type or p-type), target gas (reducing or oxidizing gas), size, and morphology.

To achieve a miniaturized CO<sub>2</sub> sensor, we have been aggressively exploring new CO<sub>2</sub> sensing materials by measuring electrical conductance in response to exposure to CO<sub>2</sub> gas. Thus, we report the possibility of using nanocrystalline TiO<sub>2</sub> doped with potassium as a resistive CO<sub>2</sub> sensing material, which we have demonstrated successfully for the detection of CO<sub>2</sub> gas. In this work, we investigated the feasibility of using K-doped TiO<sub>2</sub> nanowires for the detection of CO<sub>2</sub> gas, and the effect of the H<sub>2</sub> plasma treatment of the nanowires on their detection sensitivity.

## Experimental Methods

### Fabrication of K-doped Nanowires as Sensor Elements

We fabricated TiO<sub>2</sub> nanowires by the moisture-assisted, direct oxidation of titanium in the presence of KOH. Thin films of Ti were prepared by using a DC magnetron sputtering system. Before deposition, we used a turbo molecular pump to reduce the pressure in the chamber down to less than  $1 \times 10^{-7}$  Torr. A water-cooled Ti target, which had a diameter of 3 inches and a purity of 99.99%, was mounted at a distance of 13 cm from the substrate holder. A pure, thin film of Ti was deposited at a constant operational pressure, i.e., 5 mTorr, in Ar (99.999%) flowing at 45 sccm by heating the substrate to 400 °C. A constant DC power of 120 W was maintained. The deposition time of Ti metal thin film was 20 minutes, and the thickness of the Ti thin film was estimated to be 200 nm.

For the fabrication of the TiO<sub>2</sub> nanowires, one drop (2 mL, area of  $\sim 1 \text{ cm}^2$ ) of a 1 wt% aqueous solution of KOH (Aldrich, 99+%) was placed at the center of the Ti deposited on the substrate. Then, the substrate was inserted into a quartz tube and placed in a horizontal tube furnace (Lindberg, TF55035A) for the heat treatment. First, the tube was purged with 5% H<sub>2</sub> balanced with Ar gas flowing at a rate of 1000 mL/min for 10 min, and then the tube was heated to 150 °C at a ramping rate of 5 °C/min. After 30 min at 150 °C, the temperature of the furnace was increased at the rate of 30 °C/min to 650 °C, at which it was maintained for 4 hours in the humid Ar gas that was flowing at the rate of 50 mL/min. The humid gas was prepared by bubbling the Ar gas through DI water at room temperature. The humidity was monitored by a humidity sensor (HMP234, Vaisala), and the relative humidity of the gas was maintained at approximately 60%. After heat treatment, the sample was cooled to room temperature rapidly by air quenching to minimize the oxidation of the sample while it was cooling.

### Microstructure and XRD Analysis

After the growth of the nanowires, the samples were washed with deionized water for 24 hr until the pH reached about 7 with stirring to remove any excess KOH. Then, the samples were dried at 60 °C for 24 hr. X-ray diffraction (XRD) patterns of the products were recorded using a Scintag PAD-V diffractometer with Cu K $\alpha$  radiation at 45 kV and 20 mA in  $2\theta$ , ranging from 20° to 60°. Field emission scanning electron microscopy (FESEM, Model XL-30, Philips) images were obtained.

### Measurement of Sensing Characteristics

Sensing tests were performed by attaching Au electrodes and Au lead wires on top of the TiO<sub>2</sub> nanowires on the Al<sub>2</sub>O<sub>3</sub> substrate, as shown in Figure 1. The Au electrodes were cured at 500 °C for 1 h. The sensor was held in a tube furnace and heated

from 500 °C at different H<sub>2</sub> levels from 2% to 10%, and then CO<sub>2</sub> gas was introduced into the furnace. The response of the sensor was observed in the range of 500 to 2500 ppm of CO<sub>2</sub>, and the change in the resistance was measured at each CO<sub>2</sub> concentration.

### Condition of H<sub>2</sub> plasma treatment

To improve their sensitivity, the K-doped TiO<sub>2</sub> nanowires were treated with H<sub>2</sub> plasma at 350 °C. H<sub>2</sub> Plasma treatments were performed with ICP source frequency 2 MHz and power 30 W. The RF frequency applied to the chuck was 13.56 MHz, with the chuck power 200W. H<sub>2</sub> gas flow rate was 50 sccm. The source power controls the ion density in the plasma, while the chuck power determines the energy of ions in plasma.

## Results

### Characteristics of K-doped TiO<sub>2</sub> Nanowires

The SEM images of the nanowires obtained by the oxidation of the thin film of Ti with KOH are shown in Fig. 1.

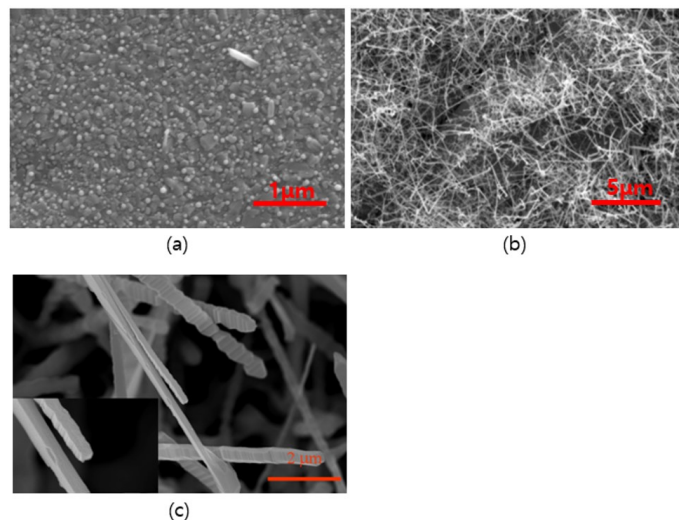


**Fig. 1** SEM images of nanowires fabricated on thin Ti film with KOH

To understand the mechanism for nanowires formation, heat-treatment was interrupted after 5 min and then surface morphology was investigated as shown in Fig. 1(a). Small islands were formed, and the separate islands grew into short nanowires. If the potassium was not continuous on the surface of Ti thin film and consisted of particles smaller than 5 nm, the K particle could have acted as a catalyst to adsorb oxygen. Therefore, the adsorption of oxygen is more predominant on K particles than others. Due to the difference of oxygen supply, the growth rate of TiO<sub>2</sub> on the K particles might be drastically faster than that

of the sides, thus causing them to survive and maintain their morphology. After 30 min heat treatment, as seen in Fig. 1(b), the Ti thin film shows well-formed nanowires that their lengths were up to 5  $\mu\text{m}$  with 5nm or less in diameter. The density of the nanowires was so high and uniform on the entire area of the substrate that many of the nanowires were made into large bundles. It is interesting to recognize that Some nanowires exhibit a rectangular cross-section while others consist of connected polyhedral, as shown in Fig. 1(c) based on ultra-high resolution SEM image.

There was no growth of the nanowires unless the KOH was used, and most of the Ti film was oxidized easily after the heat treatment. Therefore, the amount of oxygen or the oxidation sites on the thin film of Ti should be limited. KOH played an important role in the formation of the  $\text{TiO}_2$  nanowires<sup>8</sup>.

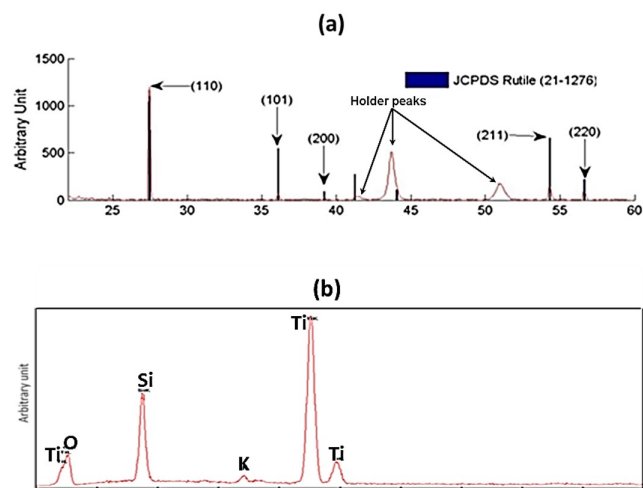
For the growth of  $\text{TiO}_2$  nanowires in a limited oxygen atmosphere, Ti always has to be available at the droplets by the diffusion of Ti. In order to check this assumption, the diffusion length of a Ti cation can be used. The chemical diffusivity ( $D$ ) of Ti cation interstitials in a single crystal rutile  $\text{TiO}_2$  in the temperature ranges of 900 ~ 1400 K was reported by Radecka et al.<sup>9</sup>, and they presented the equation of the diffusivity in the following form:

$$D = (0.001 \pm 0.4) \exp(-48.7 \pm 8 \text{ kJ/mol}) / RT \text{ cm}^2 / \text{s}$$

From equation (1), the diffusion length of titanium interstitials at 800 °C for 30 min is estimated to be 5  $\mu\text{m}$  by using  $\sqrt{Dt}$ . According to this calculation, there is enough Ti to grow nanowires on the droplets.

In related previous work, potassium iodide was used as a catalyst for the growth of tungsten oxide nanoribbons, and it was proposed that the nanoribbons grew by a vapor-liquid-solid (VLS) mechanism from a liquid K-W-O alloy<sup>10</sup>. The results of this earlier work may indicate that the likely mechanism for the growth of the K-doped  $\text{TiO}_2$  nanowires from the K-Ti-O alloy droplets was similar to that of the tungsten oxide nanoribbons from a K-W-O alloy. In general, the VLS mechanism has a eutectic reaction for the liquid phase at the temperature of the heat treatment. However, there were no caps of the catalyst at the end of the nanowires, which is a well-known characteristic of the VLS mechanism<sup>11,12</sup>. Thus, there also is the possibility of growth by the VSS (vapor-solid-solid) mechanism. On the surface of thin film of Ti, potassium can adsorb oxygen easily at the limited oxygen atmosphere, so the oxidation of the thin film of Ti is more pronounced on potassium. One-dimensional  $\text{TiO}_2$  can grow because of the role of the potassium<sup>13</sup>.

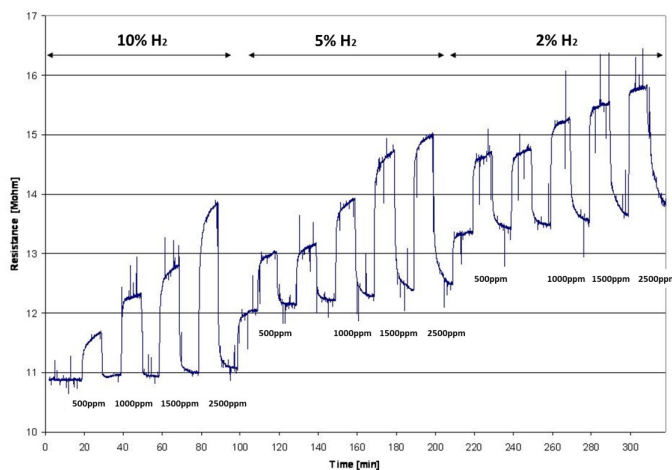
The XRD pattern indicated that the rutile phase was stable (JCPDS card: No 21-1276). The dominant peaks at 26.9°, 53.7°, and 55.8° can be assigned to rutile- $\text{TiO}_2$  (110), (211), and (220), respectively<sup>14</sup>, as shown in Fig. 2(a). A strong (110) peak indicates preferential growth along c-axis parallel to the plane.



**Fig. 2** (a) XRD pattern of the nanowires and (b) representative EDX spectrum

The XRD pattern also shows narrow and sharp peaks indicating good crystalline characteristics of the samples. Fig. 2(b) shows the data of Energy Dispersive X-ray spectroscopy (EDX) was performed in the SEM mode, and an EDX examination of the nanowires indicated that they consisted of titanium, oxygen, and potassium.

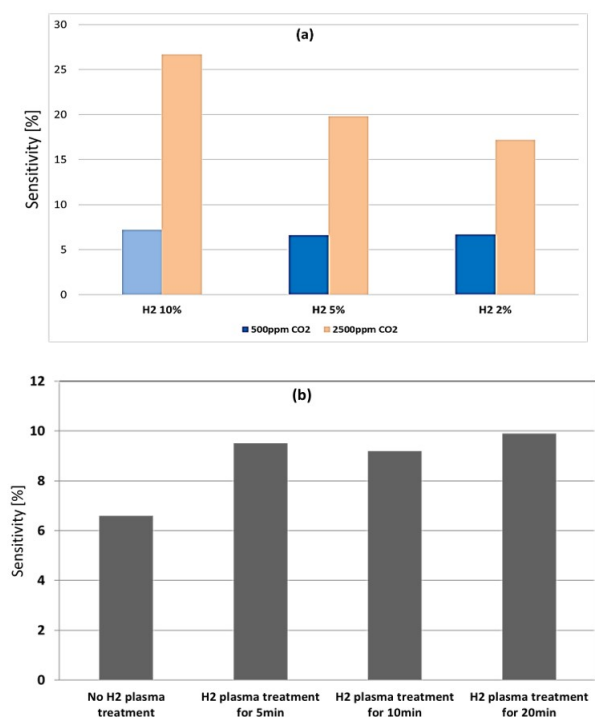
### Sensing Behaviors of K-doped $\text{TiO}_2$ Nanowires



**Fig. 3** Resistance changes of  $\text{TiO}_2$  nanowires sensor from  $\text{CO}_2$  concentration at 450 °C and the different levels of  $\text{H}_2$  background gas

Fig. 3 shows the resistance changes to the  $\text{CO}_2$  concentration from 500 ppm to 2500 ppm at 500 °C on as-grown, K-doped  $\text{TiO}_2$  nanowires. The sensing test temperature was 500 °C, and the level of the  $\text{H}_2$  background gas varied from 2% to

10%. Since the as-grown K-doped TiO<sub>2</sub> nanowires were p-type semiconductors and CO<sub>2</sub> was categorized as a reducing species, the resistance of the nanowires increases when they are exposed to CO<sub>2</sub><sup>15</sup>. The baseline of the sensors drifted slightly in air, and this observation is being investigated further. Sensitivity (S) was defined as the ratio of  $[(R_{CO_2}R_a) / R_a] \times 100$ , where R<sub>CO<sub>2</sub></sub> is the resistance of the nanowires when they are exposed to specific concentrations of CO<sub>2</sub>, and R<sub>a</sub> was measured as the resistance in air.



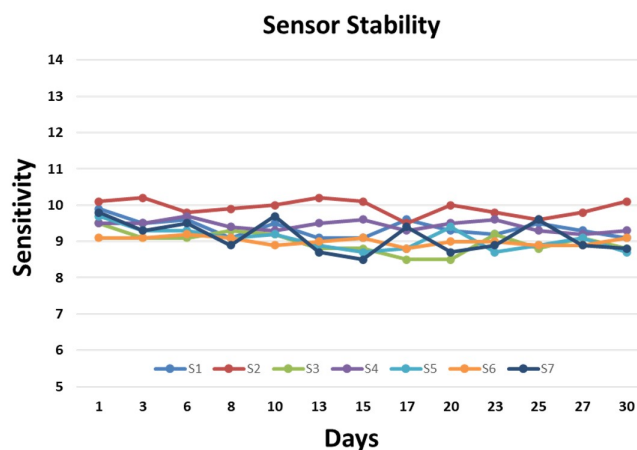
**Fig. 4** (a) The sensitivity changes of TiO<sub>2</sub> nanowire sensors at different levels of H<sub>2</sub> background gas and (b) the sensitivity changes of the sensors at post H<sub>2</sub> plasma treatment with different times

Fig. 4(a) shows the sensitivity changes of the K-TiO<sub>2</sub> nanowire sensor at sensing temperatures for different levels of H<sub>2</sub> background gas. The sensitivity is defined as the resistance of the sensor at a given concentration of the target gas (saturated R values in Figure 3) normalized by the resistance in the absence of the target gas (R<sub>0</sub>). Although the sensitivity at a CO<sub>2</sub> concentration of 500 ppm did not depend significantly on the levels of background H<sub>2</sub> gas, the sensitivity was improved by increasing the level of H<sub>2</sub> background gas at high concentrations of CO<sub>2</sub>. According to this result, hydrogen on the surface of TiO<sub>2</sub> nanowires played an important role in the absorption of CO<sub>2</sub>.

Fig. 4(b) shows the sensitivity at post H<sub>2</sub> plasma treatment with different times. The sensitivity of the as-grown nanowires was 6.6% at a CO<sub>2</sub> concentration of 500 ppm. After treatment

with the H<sub>2</sub> plasma for 5 min, the sensitivity increased from 6.6% to 9.5% at the CO<sub>2</sub> concentration of 500 ppm. The improvement of the sensitivity was not dependent on the time of the plasma treatment. After the H<sub>2</sub> plasma treatments for times ranging from 5 to 20 min, the improvements were similar. This improvement might be due to physical and chemical effects from ion bombardment, surface charges, and etching by the H<sub>2</sub> plasma<sup>16</sup>. Hydrogen ion bombardment might modify the surfaces of the nanowires and create dangling bonds that can react easily with CO<sub>2</sub> and produce hydrocarbonates on the nanowires<sup>17</sup>. The H<sub>2</sub> plasma treatment on TiO<sub>2</sub> is related to the number of oxygen vacancies and Ti<sup>3+</sup>. The H<sub>2</sub> plasma treatment might create electron-hole separation in TiO<sub>2</sub> and then enhances the surface-active states of TiO<sub>2</sub> by changing its electronic structure from TiO<sub>2</sub> (Ti<sup>4+</sup>) to Ti<sub>2</sub>O<sub>3</sub> (Ti<sup>3+</sup>). This behavior makes a positive contribution to absorbing O<sub>2</sub> ions on TiO<sub>2</sub> exposed to air, the sensitivity of the sensor can be enhanced by increasing the hole accumulation layer on the surface of TiO<sub>2</sub>.<sup>18</sup>

The sensing results reported on p-type metal oxides towards CO<sub>2</sub> are summarized in Table 1. Compared with other research about CO<sub>2</sub> sensors, the K-doped TiO<sub>2</sub> nanowire-based sensor exhibited reasonable performance about both of response/recovery time and sensitivity because of the increased surface area and the H<sub>2</sub> plasma treatment. In the case of the K-doped TiO<sub>2</sub> nanowire sensor, the 80% response time for the CO<sub>2</sub> gas was about 1~2 min, and the recovery time was less than 1 min.



**Fig. 5** Sensitivity towards 500ppm CO<sub>2</sub> for 30 days from different 7 sensors with H<sub>2</sub> plasma treatments for 20min

To prove the reproducibility of sensor assembly, seven different sensors were fabricated using the same procedure. Fig. 5 plots the sensitivity values of the sensor with H<sub>2</sub> treatment 20min towards 500ppm CO<sub>2</sub> concentration. The maximum sensitivity was 10.1 and the minimum was 9.1, with a standard deviation of 0.32. To check long-term stability, sensing behaviors were investigated for 30 days, with measurements taken every 2-3 days.

**Table 1** Summary of Material Properties and Performance in Gas Sensing

Material	Synthesis Method	Operating Temp. (°C)	Gas/ppm	Response	Response/Recovery Time (s)	Long-Term Stability/Reproducibility	Ref.
Au-functionalized CuO	Electron-beam lithography, thermal evaporation	300	CO <sub>2</sub> /2000 ppm	365%	258 s/264 s	14 days/NA	[25] <sup>19</sup>
CuO/CuFe <sub>2</sub> O <sub>4</sub>	RF sputtering	250	CO <sub>2</sub> /5000 ppm	40	3300 s/480 s	NA/NA	[26] <sup>20</sup>
SnO <sub>2</sub> -Co <sub>3</sub> O <sub>4</sub>	Sol-gel spin coating	30	CO <sub>2</sub> /2000 ppm	13.68	2 s/12 s	NA/NA	[27] <sup>21</sup>

Fig. 5 shows that the sensitivity values at 500 ppm CO<sub>2</sub> were stable during this test period. The worst sensor shows about 10% variation, however there is no continuous degradation of the sensor during the trials. Therefore, we can attribute this to natural variation and assume the sensor is operating stably for 30 days.

## Discussion

### Sensing Mechanisms

In resistive TiO<sub>2</sub> gas sensors, gas detection is based on the change in electrical resistance of TiO<sub>2</sub> in response to exposure to a targeting gas. Adsorption of gases on the surface of TiO<sub>2</sub> results in the transfer of carrier charges between the gas and the TiO<sub>2</sub>, which permits tuning of the electrical resistance. As TiO<sub>2</sub> is exposed to air, oxygen usually can be adsorbed in three forms: molecular O<sub>2</sub>, atomic O and O<sub>2</sub> species<sup>22</sup>. Once oxygen ions are chemisorbed, the concentration of free charge carriers (holes) increases in p-type materials. Chemisorbed oxygen species can form a hole-accumulating layer near the TiO<sub>2</sub> surface. When a targeting gas is introduced after chemisorption of O<sub>2</sub>, it reacts with adsorbed oxygen and may chemisorb by transferring electrons to the TiO<sub>2</sub>. Accordingly, the recombination of electron holes increases, narrowing the accumulation layer. Hence, the resistance of materials increases depending on the concentration of a targeting gas.

### Enhancement of Sensitivity

In general, one-dimensional nanostructures of metal oxides have led to more efficient chemical sensors because of their large surface areas. In addition, the sensitivity improvement also was contributed by the incorporation of the hydroxyl group (OH) on the surface of the base metal oxide sensor<sup>17</sup>. Two possible mechanisms could be explained for the sensitivity improvement by the KOH droplets. First, a local depletion area around the KOH droplets could have formed on the surface of the nanowire as a result of a charge transfer between the KOH droplets and the TiO<sub>2</sub> nanowire<sup>23</sup>. Atomic oxygen species dissociated on the KOH droplets with strong catalytic abilities could make hydroxyl ions (OH<sup>-</sup>) as reaction sites to absorb CO<sub>2</sub> onto the surface of the nanowire. The other mechanism could be

explained by the TiO<sub>2</sub> surface reaction. The surface of TiO<sub>2</sub> can react immediately with hydrogen or humid air and form hydroxyl groups. When the surface of the TiO<sub>2</sub> is fully hydroxylated, the oxide ions in the oxide and hydrogen or humid air absorbed on the surface would form hydroxyl groups<sup>24</sup>. Surface bridging hydroxyls could modulate the surface property of TiO<sub>2</sub> significantly, thereby improving its reactivity with CO<sub>2</sub>.

### Effect of Doping Metal on Sensing Behavior

Introducing noble metals such as Au, Ag, Pt, and Pd is one of the most effective and widely used methods for improving the gas sensing response in the case of metal oxide sensing materials. Firstly, adsorption activation energy is decreased, which can improve the sensing response<sup>25</sup>. Another effect of doping with another metal is that it changes the size, porosity and surface area of the metal oxide. As a result, gas molecules adsorption sites and diffusion paths are modified<sup>26</sup>. In most cases, doping with another metal causes the reduction in grain size. When the size of the grain is less than twice of the length of the Debye then the entire grain size is occupied by the electron depletion layer. Therefore, the gas sensing property of metal oxide is improved<sup>27</sup>.

### Future Research

The K-doped TiO<sub>2</sub> nanowire-based CO<sub>2</sub> microsensor is a resistor-type sensor, which can be integrated easily into a sensor array to detect various gases and to provide signals for automatic control systems. To the best of our knowledge, this is the first time it has been demonstrated that K-doped TiO<sub>2</sub> nanowire sensing material can respond to various concentrations of CO<sub>2</sub> gas in a significant and consistent way. This development creates opportunities for the fabrication of simple, inexpensive CO<sub>2</sub> microsensors with low power consumption due to their small sizes.

There are still some questions which cannot be explained by using the existing gas sensing mechanism. Therefore, it is necessary to do more research in this topic for a better understanding of the topic. In this area, more experiments are required using modern techniques such as situ analysis to know about the effect of different types of gas sensing mechanism on the performance of gas sensors. Further exploration will include

expanding the detection range of CO<sub>2</sub> concentration, reducing the operational temperature, and improving the baseline stability by understanding interference among other gases.

## Conclusion

Traditionally, transition metal oxides, such as TiO<sub>2</sub> and SnO<sub>2</sub>, have been used extensively in gas sensor applications for reactive gases such as CO and H<sub>2</sub> because of the changes in their electrical conductivities in the presence of a target gas. However, to date, limited research about a CO<sub>2</sub> sensor that uses transition metal oxide has been reported. K-doped TiO<sub>2</sub> nanowires are promising as potential CO<sub>2</sub> gas sensors. After treatment with H<sub>2</sub> plasma, the sensor showed greater sensitivity to CO<sub>2</sub> gas. Nevertheless, due to the inherent difficulties associated with working at the nanoscale, the characterization of individual nanowires are not straightforward tasks and require further research and development. Although additional research is needed to detect the variable range of CO<sub>2</sub> concentration, and to stabilize the baseline by investigating the interference with other gases including humidity, the results of this study indicate that the K-doped TiO<sub>2</sub> nanowires provide a promising opportunity for the development and use of simple, inexpensive CO<sub>2</sub> microsensors. Nanowires are one-dimensional (1D) nanostructures that have recently gained immense attention as potential morphologies for the enhancement of chemical sensing performances. Nanowires have been the subject of considerable attention in the last few years. Several characteristics of p-type metal oxide nanowires, such as high surface-area-to-volume ratios and high carrier-charge transport, make them a promising choice for the fabrication of chemical sensors. Indeed, a few problems remain, such as a lack of selectivity and high working temperatures, which require surface or bulk modification order to be resolved.

## References

- 1 <https://gml.noaa.gov/ccgg/>, *Earth system research laboratories, Global monitoring laboratory*.
- 2 K. Sahner, A. Schulz, J. Kita, R. Merkle, J. Maier and R. Moos, *Sensors*, **8**, 4774–4785.
- 3 C. Wang, L. Yin, L. Zhang, D. Xiang and R. Gao, *Sensor*, **10**, 2088–2106.
- 4 J. Maier, *Sensors and Actuators B*, **65**, 199–203.
- 5 J.-S. Lee, J.-H. Lee and S.-H. Hong, *Sensors and Actuators B*, **96**, 663–668.
- 6 I. Lee and S. Akbar, *Ionics*, **20**, 563–569.
- 7 G. Fine, L. Cavanagh, A. Afonja and R. Binions, *Sensors*, **10**, 5469–5502.
- 8 T. Zaremba and D. Witkowska, *Materials Science-Poland*, **28**, 25–41.
- 9 M. Radecka, P. Sobaś and M. Rekas, *Solid State Ionics*, **119**, 55–60.
- 10 K. Hong, W. Yiu, H. Wu and J. M. Xie, *Nanotechnology*, **16**, 1608–1611.
- 11 V. Schmidt, J. Wittemann, S. Senz and U. Gosele, *Advanced Materials*, **21**, 2681–2702.
- 12 V. Dubrovskii, G. Cirlin, N. Sibirev, F. Jabeen, J. Harmand and P. Werner, *Nano Letters*, **11**, 1247–1253.
- 13 H. Kim, H. Na, J. Yang and D. Kim, *Journal of Alloys and Compounds*, **504**, 217–223.
- 14 A. Wisitsoraat, A. Tuantranont, E. Comini, G. Sberveglieri and W. Wlodarski, *Thin Solid Films*, **517**, 2775–2780.
- 15 C. Huang, B. Huang, C. Hsiao, C. Yeh, C. Huang and Y. Jang, *Diamond Related Materials*, **17**, 624–627.
- 16 A. Prim, E. Pellicer, E. Rossinyol, F. Peiró, A. Cornet and J. Morante, *Advanced Functional Materials*, **17**, 2957–2963.
- 17 Q. Wang, Z. Guo and J. S. Chung, *Materials Research Bulletin*, **44**, 1973–1977.
- 18 S.-C. Chang, T.-H. Li and H.-T. Chan, *Int. J. Electrochem. Sci.*, **16**, 1–8.
- 19 R. Wimmer-Teubenbacher, F. Sosada-Ludwikowska, B. Travieso, S. Defregger, O. Tokmak, J. Niehaus, M. Deluca and A. A., *Chemosensors*, **6**, 56.
- 20 A. Chapelle, I. Younsi, S. Vitale, Y. Thimont, T. Nelis, L. Presmanes, A. Barnabé and P. Tailhades, *Sens. Actuators B Chem*, **204**, 407–413.
- 21 G. Joshi, J. Rajput, L. Purohit and L.P., *Microporous Mesoporous Mater*, **326**, 2–9.
- 22 H. Kim and J. Lee, *Sens. Actuators B Chem*, **192**, 607–627.
- 23 M. Arafat, B. Dinan, S. Akbar and ASMAHseeb, *Sensors*, **12**, 7207.
- 24 C.-Y. Wu, K.-J. Tu, J.-P. Deng, Y.-S. Lo and C.-H. Wu, *Materials*, **10**, 566.
- 25 R. Zhou, X. Lin and D. Xue, *Sens Actuators B*, **260**, 900–907.
- 26 H. Ji, W. Zeng and Y. Li, *Nanoscale*, **11**, 22664–22684.
- 27 H. Chen, J. Hu, G.-D. Li, Q. Gao, C. Wei and X. Zou, *ACS Appl Mater Interfaces*, **9**, 4692–4700.